Preferred citation: J.-C. Roux, J.-F. Bloch, R. Bordin and P. Nortier. The net normal force per crossing point: A unified concept for the low consistency refining of pulp suspensions. In **Advances in Pulp and Paper Research, Oxford 2009**, *Trans. of the XIVth Fund. Res. Symp. Oxford, 2009*, (S.J. I'Anson, ed.), pp 51–83, FRC, Manchester, 2018. DOI: 10.15376/frc.2009.1.51.

THE NET NORMAL FORCE PER CROSSING POINT: A UNIFIED CONCEPT FOR THE LOW CONSISTENCY REFINING OF PULP SUSPENSIONS

J.-C. Roux, J.-F. Bloch, R. Bordin and P. Nortier*

Laboratoire de Génie des Procédés Papetiers, UMR CNRS 5518, Grenoble INP-Pagora
461 rue de la Papeterie, 38402 Saint Martin d'Hères – France
Tel : +33 476 826 911 – Fax : +33 476 826 933
*Email : jean-claude.roux@grenoble-inp.fr (corresponding author)

ABSTRACT

The objectives of this article are:

– First, to theoretically propose a unified concept: the net normal force per crossing point,
– Second, to experimentally undertake refining trials on a pilot disc refiner in order to compare all concepts for the refining intensity and to validate the chosen one.

We will begin by re-visiting the old concepts of the refining intensity, in the low consistency regime. After a theoretical proof based upon the physics of the phenomena, applied to beaters and industrial refiners, a unified concept of the refining intensity is proposed and strengthened: the net normal force per crossing point.

Then, experimentations are undertaken on a pilot refiner (single disc) in hydracycle (or batch) conditions. More precisely, the effects of the grinding codes and of the average crossing angle

of the bars are analyzed in a set of 6 refining trials. For these experimentations, different engineering concepts of the refining intensity are compared (specific edge load Bs, specific surface load SSL, modified edge load MEL, net tangential force per crossing point and net normal force per crossing point). These refining intensities should allow to analysing the cutting kinetics of fibres.

All the chosen engineering concepts reach this goal more or less however the net normal force per crossing point is the best tool. Indeed, through the range of the data concerned, it revealed a clear monotonous evolution with the cutting kinetics on fibres. The more is the net normal force per crossing point, the more is the cutting effect on fibres.

1 THEORETICAL APPROACH

1.1 Case of a beater

1.1.1 Parallel bars

In the earlier 1887, Jagenberg [1] studied the case of a beater where the bars were parallel to each other and to the axis of the roll as it can be seen on figure 1. He realized that the bar contact area could have a role in quantifying the refining action on fibres. The bar contact area A_c is the real area (m^2) obtained when the bars of the roll overlap the bars located on the bedplate.

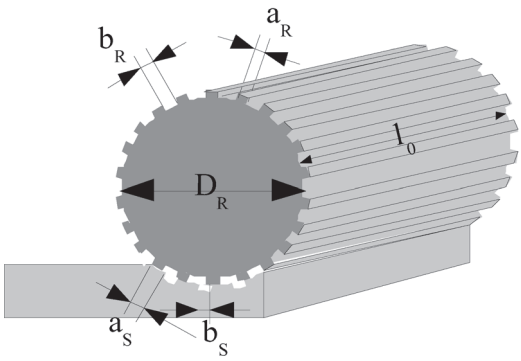

Figure 1. Geometry of a beater.

In order to calculate this engineering parameter A_c, we must begin as Jagenberg did by defining the variables appearing in figure 1. D_R is the diameter of the roll (m) and a_R, a_S are, respectively the width (m) of bars on the roll, named rotor, and the width of bars on the bedplate, named stator. l_0 is the width (m) of the bedplate; in this typical case of parallel bars beater, the width of the bedplate is the same as the common length of the bars (m) on the bedplate or stator bars. n_R and n_S are, respectively the number of bars on the roll, and on the bedplate.

Jagenberg performed the fraction of the developed area of the roll covered by the roll bars at diameter D_R, and then this term was multiplied by the area covered by the stator bars on the bedplate. This calculation gives the bar contact area A_c:

$$A_c = \frac{n_R.a_R.l_0}{\pi.D_R.l_0}.n_S.a_S.l_0 \tag{1}$$

Another expression can be obtained after simplification of the term l_0 in the fraction referring to roll parameters.

$$A_c = \frac{n_R.a_R.n_S.a_S.l_0}{\pi.D_R} \tag{2}$$

Jagenberg defined another engineering parameter as the cumulative edge length L_c since this term appears clearly in equation (2):

$$L_c = n_R.n_S.l_0 \tag{3}$$

Hence, he pointed out two engineering parameters:

– the cumulative edge length L_c (m);
– the bar contact area A_c during the overlapping of the roll in front of the bedplate.

However, he did not write the relation between these two engineering variables L_c and A_c for calculating the cumulative edge length L_c when the bar contact area A_c is known.

By introducing equation (3) in the bar contact area given by equation (2), the relation can be expressed as follows:

$$\boxed{L_c = \frac{\pi.D_R}{a_R.a_S}.A_c} \tag{4}$$

At this point of our development, it is interesting to find the expressions of n_R the number of bars on the roll and n_S the number of bars on the bedplate versus the beater variables as the bar width, a_R, a_S (m), the bar length l_0 (m) and the length of the bedplate L_s (m).

If we complete our description of the beater technology, other variables must be introduced as the width of grooves (m), both on the rotor b_R and on the stator b_S, see figure 1.

$$\begin{cases} n_R = \dfrac{\pi.D_R}{a_R + b_R} \\ n_S = \dfrac{L_s}{a_S + b_S} \end{cases} \tag{5}$$

If we replace these expressions of the bar numbers (5) in the equation (2) of the bar contact area A_c, we obtain:

$$A_c = [L_s.l_0].\frac{a_R.a_S}{(a_R + b_R).(a_S + b_S)} \tag{6}$$

This new development leads to define the bar contact area A_c from the global overlapping area given by the term between brackets. Hence, a new fraction appears and we will see in further developments that this fraction is also obtained in case of the other refining technologies as disc or conical refiners. This fraction only includes the bar width of the rotor a_R and that of the stator a_S and the groove width of the rotor b_R and that of the stator b_S.

1.1.2 Inclined bars

In 1906 and 1907, Kirchner [2] and Pfarr [3] gave an accurate calculation of the bar contact area in case of inclined bars, both on the roll (rotor) with an angle α_R and on the bedplate (stator) with an angle α_S.

$$A_c = [L_s.l_0].\frac{a_R.a_S}{(a_R + b_R).(a_S + b_S)} \tag{7}$$

Kirchner [2] hence demonstrated that the bar contact area A_c was independent of the two angular parameters of bars α_R and α_S, he obtained the equation (7) identical to equation (6) given for the case of parallel bars.

Pfarr [3] looked after an expression of the bar contact area similar to that previously given by Jagenberg in equation (2). He first calculated the bar

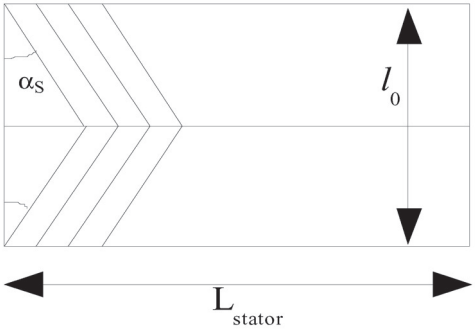

Figure 2. Geometry of the bedplate on a Valley beater.

numbers in the case of inclined bars both for the rotor and for the stator and obtained:

$$\begin{cases} n_R = \dfrac{\pi.D_R.\cos\alpha_R}{a_R + b_R} \\ n_S = \dfrac{L_s.\cos\alpha_S}{a_S + b_S} \end{cases} \tag{8}$$

Then, by introducing these bar numbers in the Kirchner's equation (7), Pfarr [3] obtained the expression of the bar contact area for the case of inclined bar beaters:

$$A_c = \frac{n_R.a_R.n_S.a_S.l_0}{\cos\alpha_R.\cos\alpha_S.\pi.D_R} \tag{9}$$

We can observe the similarity between equations (2) and (9). The last one is only an extension of the previous written by Jagenberg for the case of parallel bars beater. This can be seen by replacing the angular parameters by *0*°.

Is it possible to obtain, similarly, an extension of the cumulative edge length L_c in case of inclined bars? To answer to this question, we will use equation (4). Then, by replacing A_c given by equation (9) in the linear relation (4), it comes without any ambiguity:

$$L_c = \frac{\pi.D_R}{a_R.a_S} \cdot \frac{n_R.a_R.n_S.a_S.l_0}{\cos\alpha_R.\cos\alpha_S.\pi.D_R} \tag{10}$$

After simplification, we can obtain the expression of the cumulative edge length in case of beaters with inclined bars.

$$\boxed{L_c = \frac{n_R . n_S . l_0}{\cos \alpha_R . \cos \alpha_S}} \tag{11}$$

If we replace the angular parameters by *0*°, the previous expression already given by Jagenberg is obtained.

The cumulative edge length given by equation (11) yields three more observations.

Firstly, this cumulative edge length is found to be independent of geometrical angular parameters since the bar contact area is independent of these parameters according to Kirchner.

Secondly, the cumulative edge length is an engineering parameter previously defined [4], as the reference edge length L_{REF} (m). Hence, it is the same quantity as the cumulative edge length.

Thirdly, if l_0, the width of the bedplate is also the bar length in case of parallel bars, it is not the bar length in case of inclined bars. The real length of inclined bars (different for the rotor and for the stator) seems to appear in a complex manner as follows:

$$L_c = n_R . n_S . \frac{l_0}{\cos \alpha_R} . \frac{l_0}{\cos \alpha_S} . \frac{1}{l_0} \tag{12}$$

This is probably one reason why there were some misunderstandings in the past when different authors tried to extend the cumulative edge length from beaters to disc or conical refiners. We will use at least equation (11) to perform the calculation of the cumulative edge length for beaters, disc and conical refiners.

When α_R and α_S are different from zero angles (case of inclined bars), during the relative motion of the roll in front of the bedplate, a certain number of crossing zones are generated. Kirchner [2] named these zones "crossing points" and decided to calculate their number N_{CP}. He gave the expression of the area of a single bar crossing point (m^2) when the bar angle is known:

$$A_{CP} = \frac{a_R . a_S}{\sin(\alpha_R + \alpha_S)} \tag{13}$$

Then, the calculation of the number of crossing points N_{CP} was obtained by the ratio of the bars contact area A_c by equation (9) by the area of a single bar

crossing point A_{CP} by equation (13). The expression of N_{CP} is also given in Baker's book [5] in chapter 2.

$$N_{CP} = \frac{n_R.n_S.l_0}{\pi.D_R}.(\tan\alpha_R + \tan\alpha_S) \tag{14}$$

Again, we developed another relationship between the number of crossing points N_{CP} and the cumulative edge length L_c, with the same assumptions concerning the angles. It is possible to obtain:

$$\boxed{N_{CP} = \frac{L_c}{\pi.D_R}.sin(\alpha_R + \alpha_S)} \tag{15}$$

1.1.3 Inclined bars: net normal force per crossing point

Roux and his co-workers [4] introduced the concept of net normal force (N) and refining intensity (N) for a beater. They calculated the net normal force by the following formula which includes the global friction coefficient *f*:

$$F_n^{net} = \frac{P_{net}}{f.\pi.D_R.N} \tag{16}$$

In equation (16), P_{net} is the net power consumed by the refiner and N is the rotation speed of the rotor. Now, dividing the net normal force by the number of crossing points N_{CP}, as given by equations (14) or (15), it was possible to quantify the net normal force per crossing point.

From equation (14), we obtain the following expression of the net normal force per crossing point given by equation (17):

$$\frac{F_n^{net}}{N_{CP}} = \frac{P_{net}}{f.[n_R.n_S.l_0.(\tan\alpha_R + \tan\alpha_S)].N} \tag{17}$$

The expression between brackets in the denominator was empirically introduced by Meltzer [6], as the "extended edge length". He considered "the projected bar length as the efficiency of a bar to cross counterbars". Our theoretical approach naturally introduces the concept of extended edge length already proposed by Meltzer and then adds to its legitimacy.

The net normal force per crossing point is our candidate for describing the refining intensity in the low consistency refining process of pulp suspensions.

If the equation (15) is chosen to quantify the number of crossing points

N_{CP}, then a new expression of the net normal force per crossing point can be found, given by equation (18).

$$\boxed{\frac{F_n^{net}}{N_{CP}} = \frac{P_{net}/(L_c.N)}{f.sin(\alpha_R + \alpha_S)}} \tag{18}$$

It is noted that the numerator is simply the Specific Edge Load, B_s, (J/m or N) defined lately by Brecht and Siewert [8].

However, as the cumulative edge length and the reference edge length are the same physical quantity, the specific edge load is also the same quantity as the reference specific edge load, already introduced in [4]. Again, this adds legitimacy to the concept of the reference specific edge load that is exactly the same as the specific edge load.

However, we must admit that the specific edge load is not sufficient to adequately describe the refining intensity since two adding parameters are influencing variables in equation (18):

- the global friction coefficient f of the pulp versus bar materials;
- the sinus of the bar crossing angle given by the algebraic sum $\alpha_R + \alpha_S$.

1.2 Disc refiner analysis

1.2.1 The cumulative edge length

The extrapolation of the cumulative edge length was proposed in 1958 by Wultsch and Flucher [7]. They introduced the following well known expression [5], to calculate the cumulative edge length per revolution (m):

$$L = n_R.n_S.\bar{l} \tag{19}$$

A new variable $\bar{l}$ was introduced: the average bar length (m). Their understanding was based upon a proposed extension of Jagenberg's equation (3) as stated in Baker's book [5].

Later, Brecht and Siewert [8] used the expression (19) to calculate the Specific Edge Load B_s (J/m) by equation (20), following the initial ideas of Wultsch and Flucher:

$$B_s = \frac{P_{net}}{L.N} \tag{20}$$

However, our understanding of the cumulative edge length for disc refiners is somewhat different. At first glance, we already demonstrated in this article

that the extension of the cumulative edge length for the beaters in case of inclined bars was given by equation (11). This last one differs from equation (19) where the average bar length $\bar{l}$ is not clearly defined.

We propose to clarify the concept of the cumulative edge length, in the case of a disc refiner, through a physical analogy between a slice of the beater and an elementary annulus of disc.

On figure 3, the pulp suspension motion in the beater occurs in the plane formed by two unit vectors ($\overrightarrow{i_\rho}$, $\overrightarrow{i_\psi}$), perpendicular to the roll axis. Now, if we consider a slice of the beater in the direction of the unit vector $\overrightarrow{i_z}$, it means that the width of the bedplate is also the width of the slice beater dl_0. The determination of the elementary cumulative edge length dL_c for this slice of the beater is given by equation (11) written in a differential form as follows:

$$dL_c = \frac{n_R . n_S . dl_0}{\cos\alpha_R . \cos\alpha_S} \tag{21}$$

For a beater, the bar numbers are independent of the slice of the beater as mentioned previously. So, the integration of equation (21) is easy to perform with this type of technology and leads to equation (11) already mentioned through a global understanding at the beginning of this article.

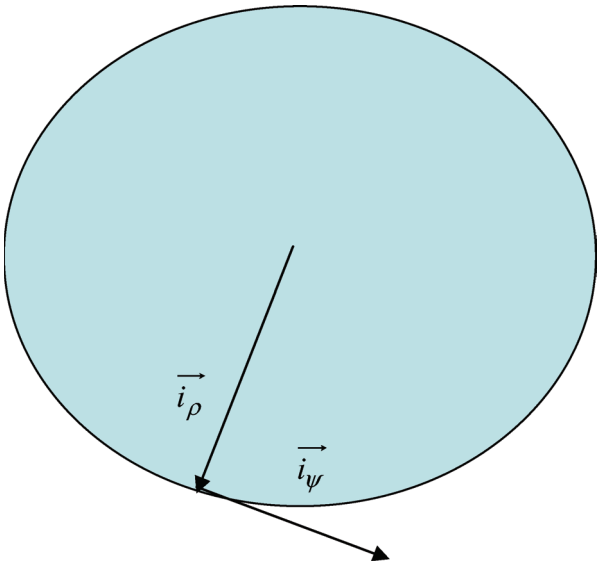

Figure 3. Slice of a beater.

On figure 4, we drew an elementary annulus comprised between the radius ρ and the radius $\rho + d\rho$. The pulp suspension motion is supposed to be circular with this type of disc refiner in the direction of the unit vector $\overrightarrow{i_\psi}$, for each radius, analogous to the case of a beater.

However, the major difficulty with a disc refiner is given by the different situations that occur with time during the relative motion of the rotor disc in front of the stator disc.

In that case, how the bar angles for both the rotor and the stator, may be defined? If one expression must be used for extrapolation, it should be that given by equation (21), which is certainly not yet currently used in the industrial practice.

A careful consideration of the disc geometry, as it was done for example in [9], can lead to the local determination of the numbers of bars on the rotor n_R and on the stator n_S as function of the local radius ρ with the corresponding

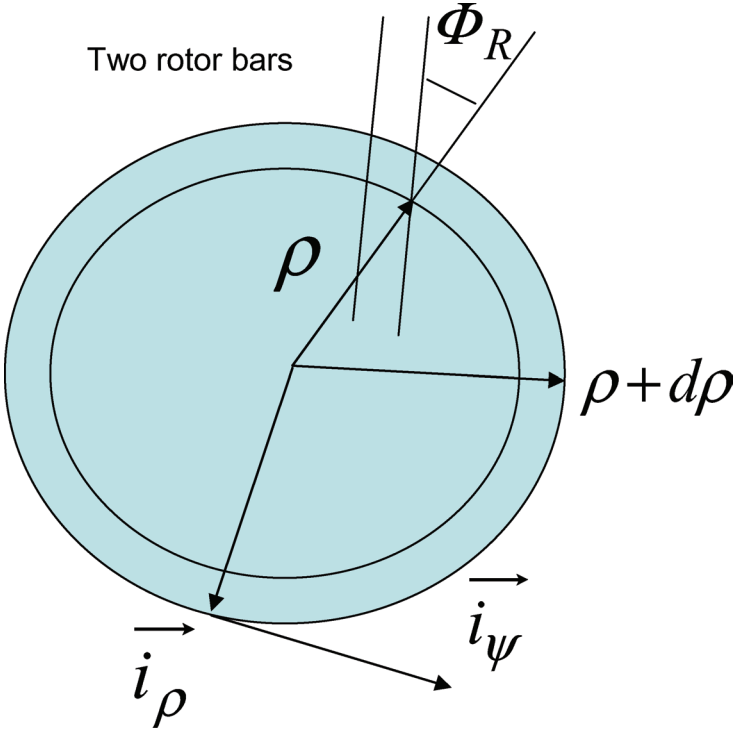

Figure 4. Elementary annulus of a disc plate for a disc refiner $\rho_i \leq \rho \leq \rho_e$.

angles Φ_R and Φ_S for the bar inclinations for the rotor and the stator, respectively:

$$\begin{cases} n_R(\rho) = \dfrac{2.\pi.\rho.cos(\Phi_R)}{a_R + b_R} \\ n_S(\rho) = \dfrac{2.\pi.\rho.cos(\Phi_S)}{a_S + b_S} \end{cases} \tag{22}$$

An analogous form of equation (21), between a slice of the beater and an annulus of a disc refiner leads to the calculation of the elementary cumulative edge length, by substituting dl_0 by $d\rho$.

$$dL_c(\rho) = \frac{n_R(\rho).n_S(\rho).d\rho}{cos\,\Phi_R.cos\,\Phi_S} \tag{23}$$

Hence, in order to find the expression of the cumulative edge length for a disc refiner, integration must be performed over the refining annulus, limited by the internal radius ρ_i (m) and the external radius ρ_e (m), using equations (22) and (23).

$$L_c = \int_{\rho_i}^{\rho_e} \frac{n_R(\rho).n_S(\rho).d\rho}{cos\,\Phi_R.cos\,\Phi_S} = \frac{4.\pi^2.\left(\rho_e^3 - \rho_i^3\right)}{3.(a_R + b_R).(a_S + b_S)} \tag{24}$$

Some observations can be given. Equation (24) reveals that L_c is independent of the bar angles on the rotor and on the stator. It confirms the result already obtained by Kirchner when beaters with inclined bars were considered, see equation (11).

The cumulative edge length is the same physical quantity as the reference edge length already introduced in [9], since it appeared naturally in the calculations. However, in this article, it is demonstrated through a physical analogy between beaters and disc refiners. The correct extrapolation of equation (11) for beaters to industrial disc refiners and their complex geometry is given by equation (24).

If we follow the equation (19) for the practical calculation of the cutting edge length, we should evaluate this quantity by the following:

$$CEL = \sum_{k=1}^{p} n_{Rk}.n_{Sk}.\Delta\rho_k \tag{25}$$

In this expression, the disc corona is divided in p elementary annulus where

the determination of the bar numbers on the rotor n_{Rk}, on the stator n_{Sk} is performed for each annulus. All these numbers are then combined in order to give the cutting edge length (*CEL*) according to equation (25).

Due to differences in case of inclined bars between the practical determination of the *CEL* given by the formula (25) and real measurements, the Stock Preparation TAPPI Committee decided to include some cosines terms in the expression (25). The next expression (26) is given for example, in the Technical Information Papers of the TAPPI Association for the determination of the cutting edge length (*CEL*):

$$CEL = \sqrt{\frac{\sum_{k=1}^{p} n_{Rk}^2 . \Delta\rho_k}{cos\left(\overline{\Phi_R}\right)}} \sqrt{\frac{\sum_{k=1}^{p} n_{Sk}^2 . \Delta\rho_k}{cos\left(\overline{\Phi_S}\right)}} \tag{26}$$

In this last equation, average angles for the rotor and the stator are empirically introduced, which could give an expression "close to" our theoretical solution.

However, we suggest using the proposed equation (24) which has some theoretical justification instead of the empirical expression, given by equation (26). Furthermore, in the TAPPI expression, both set variables are gathered angular and non angular parameters.

In the proposed equation (24), no reference is made to angular parameters, so we need to complete our physical analysis to "naturally" introduce these angular parameters, this will be done in the next paragraph.

1.2.2 The net normal force per crossing point

Equation (16) gives the net normal force versus the net power consumed for a beater; this expression includes a tangential velocity in the denominator. If one wants to develop a similar tangential velocity equation for a disc refiner; we must find its equivalent diameter or radius.

This can be done by calculating, over the disc annulus, the average tangential velocity defined as follows [10]:

$$2.\pi.<\rho>.N = \frac{\int_{\rho_i}^{\rho_e} 2.\pi.\rho.N.2\pi\rho.d\rho}{\pi.\left(\rho_e^2 - \rho_i^2\right)} \tag{27}$$

Hence, the average radius $<\rho>$ (m) is given by the expression:

$$< \rho >= \frac{2.\left(\rho_e^3 - \rho_i^3\right)}{3.\left(\rho_e^2 - \rho_i^2\right)} \tag{28}$$

Dividing the net normal force by the number of crossing points requires the determination of this last number. Due to complex geometrical situations occurring in the rotating motion of the rotor in front of the stator, it is only an average calculation of this number which is performed.

The average number of crossing points N_{CP} was already calculated by Roux [9] and its expression reduced to a simplified one in the case of a small sector angle:

$$N_{CP} = \frac{\pi.\left(\rho_e^2 - \rho_i^2\right)}{\left(a_R + b_R\right).\left(a_S + b_S\right)}.sin\left(\overline{\Phi_R} + \overline{\Phi_S}\right) \tag{29}$$

Now, the last step is the determination of the net normal force per crossing point, calculated on the average, for a disc refiner, by introducing the average radius – equation (28) and the average number of crossing points – equation (29), we finally obtain:

$$\boxed{\frac{F_n^{net}}{N_{CP}} = \frac{P_{net}}{f.\pi.2.< \rho >.N.N_{CP}} = \frac{P_{net}/\left(L_c.N\right)}{f.sin\left(\overline{\Phi_R} + \overline{\Phi_S}\right)}} \tag{30}$$

Again, some observations can be drawn. The numerator of the net normal force per crossing point is the reference specific edge load or the specific edge load since these variables express the same physical quantity: the net energy per unit length of bar edge (J/m) or (N).

This quantity: the numerator does not contain any angular parameter. These last variables are included in the denominator. In the previous TAPPI expression (26), all the variables were gathered but, in fact, there are decoupled in equation (30).

The physical analogy obtained between equations (18) and (30) is the clear demonstration that the refining intensity chosen as the net normal force per crossing point is a unified concept.

It can be applied to different technologies as a beater or an industrial disc refiner with different geometries.

The case of a conical refiner, not treated here, may be treated exactly in the same way.

2 INTERPRETATIONS OF THE INDUSTRIAL PARAMETERS

2.1 Description of the refining installation

The refining trials were undertaken on our Laboratory pilot installation [10, 11], as described on figure 5. The pilot is equipped with a single disc refiner (SD) running in hydracycle mode.

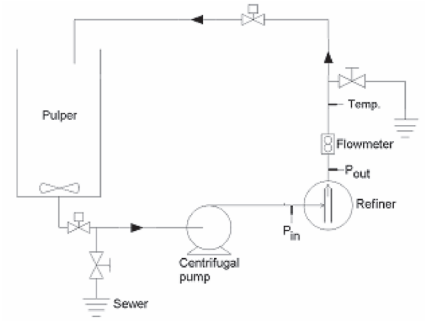

Figure 5. Laboratory refining installation.

It means that the refining energy is distributed to the pulp suspension in cycles. The refiner is an automated process with gap clearance sensor and axial force sensor. This specific metrology was previously described in [12] and will not be detailed in this article. It allows us to measuring the normal and tangential forces and to deducing both the global friction coefficient.

In order to define the different engineering parameters which will be modified during the set of refining trials, we must first remind the geometrical configuration of a disc plate, as shown on figure 6.

In this typical design, a given sector is composed of parallel bars in an annulus comprised of an internal radius ρ_i and an external radius ρ_e. On this drawing, the sector has an angular periodicity of *6* per revolution meaning that the sector angle is equal to $\theta = 60°$. Usually, the sector angle is common for the rotor and the stator. On figure 6, the angle of the first bar, located at the right side, is named the "grinding angle" and written by convention: α for the rotor disc and β for the stator disc. The understanding of the angular parameters is the same for the rotor or the stator in a first glance.

Depending on the bar chosen for the rotor disc, the bar inclination angle is varying from α to $\alpha + \theta$. Hence, a typical value of the bar inclination angle,

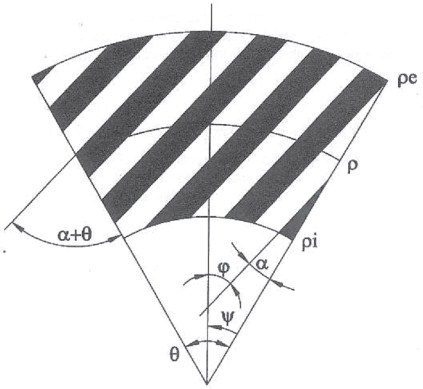

Figure 6. Geometrical patterns of a sector on a disc plate.

for each sector (rotor or stator) is given by the average value, we then obtain the following expressions:

$$\begin{cases} \overline{\Phi_R} = \alpha + \dfrac{\theta}{2} \\ \overline{\Phi_S} = \beta + \dfrac{\theta}{2} \end{cases} \tag{31}$$

If a rotor plate is superimposed in front of a stator plate, by considering the average value for each plate, the angle of the bar crossings is defined as follows:

$$\overline{\gamma} = \overline{\Phi_R} + \overline{\Phi_S} \tag{32}$$

On the one hand, the quantification of the average angle for the entire bar crossings is obtained by replacing the terms of equations (31) in equation (32):

$$\overline{\gamma} = \alpha + \beta + \theta \tag{33}$$

On the other hand, the number of bars located at a given radius ρ_k can be analytically calculated, by introducing the previous angles $\overline{\Phi_R}$ and $\overline{\Phi_S}$ in the following expressions given for the rotor, then for the stator:

$$\begin{cases} n_{Rk} = \dfrac{2.\pi.\rho_k.cos\left(\overline{\Phi_R}\right)}{a_R + b_R} \\ n_{Sk} = \dfrac{2.\pi.\rho_k.cos\left(\overline{\Phi_S}\right)}{a_S + b_S} \end{cases} \tag{34}$$

2.2 Description of the refining conditions

The pulp suspension tested in these investigations was a market pulp of non bleached Kraft Canadian softwood. Neither the characterization of the pulp nor the essence was undertaken since our aim in this article was based upon an assessment of engineering parameters.

During the six refining trials, the dry mass of the pulp in the tank was the same at $m = 14\ kg$ and the solid consistency chosen at $C = 3.5\%$ (or $35\ kg/m^3$). A constant volumetric flow measured by the flow meter was kept at $Q = 10\ m^3/h$. Hence, the time period of a cycle was constant at $V/Q = 2.4\ min$ (or $144\ s$).

The refining trials were undertaken on the same single disc refiner with the following engineering parameters: internal radius $\rho_i = 0.065\ m$; external radius $\rho_e = 0.150\ m$. These values allow the calculations of the ratio k of the internal to the external radius of the annulus:

$$k = \frac{\rho_i}{\rho_e} = 0.433 \tag{35}$$

and that of the average radius $< \rho >$, considering the equation (28) rewritten by using the previous ratio:

$$< \rho >= \frac{2.\left(1 - k^3\right)}{3.\left(1 - k^2\right)}.\rho_e = 11.31\ 10^{-2}\ m \tag{36}$$

The net power was kept constant during one refining trial. The rotation speed of the refiner was also taken at a constant value for all the refining trials: $N = 1500\ rev/min$ or 25 rev/s.

For the disc plates, made of stainless steel, the groove depth was constant at $6.4\ mm$, corresponding to a grinding code of either (*2-2-4*) or (*3-3-4*) expressed classically in sixteenth of inches. We remind to our reader that the grinding code is classically a set of *3* numerical values (*a-b-c*), respectively:

the bar width, the groove width and the groove depth (or the bar height). (*2-2-4*) is often used for short fibres and (*3-3-4*) privileges long fibres.

The sector angle was also the same during all the refining trials, a common value for both rotor and stator disc was chosen at $\theta = 22.5°$, leading to an angular periodicity of *16* sectors per revolution for one disc plate.

2.3 Description of variable engineering parameters

The engineering parameters chosen for these investigations were:

– the common value of the bar width and groove width: $a = b$;
– the net power constant during one given trial P_{net};
– the sum of the grinding angle of the rotor and the stator: $\alpha + \beta$.

In table 1, we have gathered these different numerical values, completed by the average crossing angle $\bar{\gamma}$, given by equation (32):

Table 1. Description of the chosen engineering parameters in the refining trials

Trial n°	$a = b$ *[mm]*	P_{net} *[kW]*	$\alpha + \beta$ *[°]*	$\bar{\gamma} = \alpha + \beta + \theta$ *[°]*	$\overline{\phi_R}$ *[δ]*	$\overline{\phi_S}$ *[°]*
1	3.2	16.6	0	22.5	16.25	6.25
2	3.2	9.6	0	22.5	16.25	6.25
3	4.8	12	25	47.5	21.25	26.25
4	4.8	7	25	47.5	21.25	26.25
5	4.8	12.4	0	22.5	16.25	6.25
6	4.8	24	0	22.5	16.25	6.25

The sum of the grinding angles $\alpha + \beta$ was chosen for two different numerical values:

– a so-called "cutting" geometry where $\alpha = + 5°$ and $\beta = - 5°$;
– a so-called "fibrillating" geometry where $\alpha = + 10°$ and $\beta = + 15°$.

As it was previously mentioned in [9], the refining intensities defined by different authors in the paper literature are always proportional to the net power applied. The bar width a and the average angle $\bar{\gamma}$ of the bar crossings are also known to be influent variables for characterizing the refining effects on fibres.

2.4 Determination of different refining intensities

For all the refining trials specified by table 1, we propose to calculate the different refining intensities in the following order: the specific edge load [8], the specific edge load recommended according to the TAPPI engineering rules, the specific surface load [13], the modified edge load [6], the net tangential force per crossing point [9], the net normal force per crossing point [9].

2.4.1 Determination of the specific edge load

If we combine equations (20) and (24) with the correct quantification of the cumulative edge length, the determination of the specific edge load B_s is then given by the following expressions:

$$\boxed{B_s = \frac{P_{net}}{L_c.N} = \frac{3.(a+b)^2.P_{net}}{4.\pi^2.\left(\rho_e^3 - \rho_i^3\right).N}} \tag{37}$$

Two different bar widths (or groove widths) and six different net powers lead to consider a refining intensity in a range of *1* to *5.6*.

2.4.2 Determination of the specific edge load according to TAPPI rules

As it is proved in this article, no angular parameter can be found in equation (37). TAPPI rules proposed to empirically introduce the angular parameters as described in the following developments:

$$\begin{cases} B_{s-TAPPI} = \dfrac{P_{net}}{CEL.N} \\ CEL = \sqrt{\dfrac{\sum_{k=1}^{p} n_{Rk}^2.\Delta\rho_k}{cos\left(\overline{\Phi_R}\right)}}\sqrt{\dfrac{\sum_{k=1}^{p} n_{Sk}^2.\Delta\rho_k}{cos\left(\overline{\Phi_S}\right)}} \end{cases} \tag{38}$$

According to these rules, the calculation of the specific edge load can be done after the primary determination of the edge length both for the rotor EL_R and the stator EL_S.

The edge length for the rotor and the stator are the respective expressions under square root signs in equations (38). For sake of simplification, we consider that the bar width *a*, respectively the groove width *b*, are the same for the rotor and the stator. In equations (38), the disc corona is divided in *p*

elementary annulus. The edge length for the rotor EL_R can be determined with the help of equation (34) that counts the bar number on a given annulus:

$$EL_R = \frac{\sum_{k=1}^{p} n_{Rk}^2 . \Delta\rho_k}{cos\left(\overline{\Phi_R}\right)} = \sum_{k=1}^{p} \frac{4.\pi^2 . \rho_k^2 . cos\left(\overline{\Phi_R}\right) . \Delta\rho_k}{(a+b)^2} \tag{39}$$

The calculation of the edge length for the stator EL_S is formally the same as that for the rotor. If a continuous expression is preferred rather than a discrete one, the cutting edge length *CEL* is then given by the following equation after integration over the global corona:

$$CEL = \frac{4.\pi^2 . \left(\rho_e^3 - \rho_i^3\right)}{3.(a+b)^2} . \sqrt{cos\left(\overline{\Phi_R}\right) cos\left(\overline{\Phi_S}\right)} \tag{40}$$

This last expression allows the final determination of the specific edge load according to TAPPI rules:

$$\boxed{B_{s-TAPPI} = \frac{B_s}{\sqrt{cos\left(\overline{\Phi_R}\right) . cos\left(\overline{\Phi_S}\right)}}} \tag{41}$$

This expression empirically introduces the angular parameters that combine grinding angles and the sector angle as previously given by equations (31).

2.4.3 Determination of the specific surface load

Lumiainen [13] claimed that the bar width and the average crossing angle must be taken into account for a more precise quantification of the refining intensity. He also gave the general formula to calculate the specific surface load:

$$SSL = \frac{B_s}{a_R + a_S} . 2 . cos\left(\overline{\gamma} / 2\right) \tag{42}$$

In case of the same bar width for the rotor and the stator, the formula is simplified to the following expression:

$$\boxed{SSL = \frac{B_s}{a} . cos\left(\overline{\gamma} / 2\right)} \tag{43}$$

All the engineering parameters are empirically included in this definition of the refining intensity.

2.4.4 Determination of the modified edge load

With this refining intensity given by Meltzer [6], the modified edge load includes the bar width, the groove width and the average crossing angle as it is expressed in the general case:

$$MEL = \frac{B_s}{2.tan\left(\overline{\gamma}/2\right)}.\left(\frac{a+b}{a}\right) \tag{44}$$

When the bar width and the groove width are the same, this equation can be simplified and the bar width then disappears, it only remains in the expression of the specific edge load B_s:

$$\boxed{MEL = \frac{B_s}{tan\left(\overline{\gamma}/2\right)}} \tag{45}$$

2.4.5 Determination of the net tangential force per crossing point

This quantity can be obtained in two steps. Firstly, the net tangential force is deduced from the net power applied and the average tangential velocity as expressed by equation (27):

$$F_t^{net} = \frac{P_{net}}{2.\pi.<\rho>.N} \tag{46}$$

Secondly, the average number of crossing points is calculated precisely with the following equations already given by Roux in [9]:

$$\begin{cases} N_{CP} = \dfrac{\pi.\left(\rho_e^2 - \rho_i^2\right)}{(a_R + b_R).(a_S + b_S)}.sin\left(\gamma^*\right) \\ sin\left(\gamma^*\right) = sin\left(\overline{\gamma}\right).\left(\dfrac{sin(\theta/2)}{\theta/2}\right)^2 \end{cases} \tag{47}$$

After replacement of the average number of crossing points in the expression of the net tangential force per crossing point, we obtain the following equation which can be practically used to calculate the required value:

$$\frac{F_t^{net}}{N_{CP}} = \frac{B_s}{sin(\gamma^*)} \tag{48}$$

2.4.6 Determination of the net normal force per crossing point

The authors of this article have theoretically demonstrated that the unified concept for quantifying the refining intensity was the net normal force per crossing point. In fact, it means that a physical term is lacking, this term is the global friction coefficient *f*. The expression of the net normal force per crossing point hence comes:

$$\frac{F_n^{net}}{N_{CP}} = \frac{B_s}{f.sin(\gamma^*)} \tag{49}$$

2.4.7 Observations on the different refining intensities

Some general observations can be drawn after calculation of the different candidates for the refining intensity. All the refining intensities, except the specific edge load, incorporate angular parameters. The specific surface load includes one more engineering parameter: the bar width on the average. The modified edge load includes the bar width and the groove width.

However, the net normal force per crossing point incorporates a new physical quantity that has never been introduced before (except by the authors themselves): the global friction coefficient.

Our last step is then to calculate the candidates for quantifying the refining intensity on fibres during the pulp refining in low consistency regime.

2.5 Calculation of different refining intensities

We have gathered all the empirical and physical quantities in table 2 in order to see if they are classified in the same order for the 6 refining trials undertaken on our pilot.

Some observations can be given. First, the star angle γ^* is very close to the average crossing angle $\bar{\gamma}$ as it can be seen through a comparison between the numerical values for all the six refining trials in tables 1 and 2. Second, the cutting speed $L_c.N$ shares the refining trials in two categories: (*1,2*) and (*3,4,5,6*) whereas the average number of crossing points N_{CP} leads to three categories: (*1,2*), (*3,4*), (*5,6*). At this point, we can observe that the level of discrimination is better by using concepts that incorporate angular parameters.

Table 2. Calculation of the different refining intensities

Trial n°	*a [mm]*	P_{net} *[kW]*	γ^* *[°]*	*f*	$L_c.N$ *[km/s]*	N_{CP}	B_s *[J/m]*	B_{sTappi} *[J/m]*	*SSL* $[J/m^2]$	*MEL [J/m]*	F_t^{net}/N_{CP} *[N]*	F_n^{net}/N_{CP} *[N]*
1	3.2	16.6	22.2	0.15	25.296	537.91	0.656	0.672	202.7	3.299	1.737	11.58
2	3.2	9.6	22.2	0.18	25.296	537.91	0.380	0.388	117.2	1.908	1.005	5.58
3	4.8	12	46.7	0.20	11.243	460.60	1.067	1.167	205.1	2.426	1.466	7.33
4	4.8	7	46.7	0.25	11.243	460.60	0.623	0.681	119.7	1.415	0.855	3.42
5	4.8	12.4	22.2	0.13	11.243	239.07	1.103	1.129	227.1	5.545	2.919	22.45
6	4.8	24	22.2	0.16	11.243	239.07	2.135	2.185	439.6	10.73	5.651	35.32

Third, for all the refining trials undertaken, the different chosen refining intensities cover a range of *1* to *6*, which is sufficiently representative for a bench-mark.

Fourth, the best discriminating refining intensities among the six candidates are given by the three last columns. This result is proved when one wants to classify the trial numbers from the smallest to the highest refining intensity; we obtain for the six different candidates:

Table 3. Classification of the refining trials by increasing the refining intensity

Refining Intensity	*Classification of the trial numbers towards increasing intensity*
B_s	2 < 4 < 1 < 3 < 5 < 6
$B_{s\text{-Tappi}}$	2 < 1 < 4 < 5 < 3 < 6
SSL	2 < 4 < 1 < 3 < 5 < 6
MEL	4 < 2 < 3 < 1 < 5 < 6
F_t^{net}/N_{CP}	4 < 2 < 3 < 1 < 5 < 6
F_n^{net}/N_{CP}	4 < 2 < 3 < 1 < 5 < 6

If we remind that the specific edge load, its calculation according to TAPPI engineering rules and the specific surface load are empirical concepts, we are not surprised by the results obtained. None of this candidate leads to the same classification as the others.

So, it is clear that these tools should be used with great care for a quantification of the refining effects on fibres, specially the shortening effect on fibres.

3 PRACTICAL RESULTS

3.1 Cutting kinetics of fibres

Among the main refining effects, the cutting on the fibres is more directly related to the refining intensity. Hence, the refining intensity concept was first developed in order to quantify this shortening effect on fibres. Our purpose is to find the refining intensity which would be the best tool to quantify the cutting kinetics on fibres, among the six possible refining intensities presented in this article.

3.2 Experimental results

For one given refining trial, the average weighted fibre length L_f was measured with a Morfi analyser at different times, which means at different specific

energies consumed by the pulp. The six refining trials are performed with a constant net power applied P_{net} and a constant rotation speed N as it was previously presented in paragraph 2.2. The following tables summarise the data obtained for the six refining trials.

Table 4. Pulp properties versus net specific energy for refining trial n°1

Pulp property	E_{sp}^{net} *[kWh/T]*			
	0	*63.4*	*146.8*	*192.2*
L_f [mm]	2.158	2.034	1.840	1.739
°SR	15	18	27	38
WRV [g/100g]	108	129	150	162

Table 5. Pulp properties versus net specific energy for refining trial n°2

Pulp property	E_{sp}^{net} *[kWh/T]*			
	0	*88.6*	*168.5*	*258.8*
L_f [mm]	2.158	2.094	1.959	1.820
°SR	15	19.5	28.5	43
WRV [g/100g]	108	133	152	167

Table 6. Pulp properties versus net specific energy for refining trial n°3

Pulp property	E_{sp}^{net} *[kWh/T]*			
	0	*87.9*	*176.7*	*266.5*
L_f [mm]	2.158	2.103	1.900	1.692
°SR	15	19.5	31.5	52.5
WRV [g/100g]	108	143	165	186

Table 7. Pulp properties versus net specific energy for refining trial n°4

Pulp property	E_{sp}^{net} *[kWh/T]*			
	0	*104.4*	*201.7*	*276*
L_f [mm]	2.158	2.118	2.003	1.868
°SR	15	20	31.5	43
WRV [g/100g]	108	144	165	176

Table 8. Pulp properties versus net specific energy for refining trial n°5

Pulp property	E_{sp}^{net} *[kWh/T]*			
	0	*89.2*	*180*	*267.8*
L_f [mm]	2.158	1.855	1.478	1.021
°SR	15	20	40	70
WRV [g/100g]	108	135	163	192

Table 9. Pulp properties versus net specific energy for refining trial n°6

Pulp property	E_{sp}^{net} *[kWh/T]*			
	0	*88.5*	*180*	*258*
L_f [mm]	2.158	1.623	1.138	0.896
°SR	15	21	45	63
WRV [g/100g]	108	137	163	181

In this article, we will only investigate on the cutting effect on fibres and will analyse the other main effects (fibrillation and hydration) in future publications.

All results can be condensed in the same figure for an assessment of the cutting kinetics on fibres for all the experimental trials performed.

3.3 Empirical modelling of the cutting kinetics

For the range of specific energy concerned by these refining trials, a second order model fits adequately the experimental average weighted fibre length. Hence, the following equation applies with a good precision for all the refining trials performed. For the refining trial n°k:

$$L_{f-k} = a_k.\left(E_{sp}^{net}\right)^2 + b_k.\left(E_{sp}^{net}\right) + L_{f0} \tag{50}$$

This empirical model is then used to interpolate the average weighted fibre length L_{f-k} (for the refining trial n° k) at the same net specific energy consumption chosen: *150 kWh/T*.

All the calculated data are summarised in table 10.

Table 10. Interpolation of the average weighted fibre length L_{f-k} for $E_{sp}^{net} = 150\ kWh/T$ and for the six refining trials

Trial n°k; k	*1*	*2*	*3*	*4*	*5*	*6*
$10^{+6}.a_k$	–0.458	–2.546	–4.971	–3.863	–4.992	+7.979
$10^{+4}.b_k$	–20.42	–6.646	–4.521	+0.142	–29.03	–69.82
r_k^2	0.9987	0.9932	0.9917	1.0000	1.0000	0.9999
L_{f-k}(150kWh/T) [mm]	1.841	2.001	1.978	2.073	1.610	1.290

The refining trial number *6* was performed with the highest refining intensity as it is proved by table *3*, whatever the candidate used for defining this refining intensity. The positive sign of the coefficient a_6 means a change in the curvature of the cutting kinetics on fibres, compared to the other coefficients, from a_1 to a_5, as it can be observed on figure 7.

With table 10, the six refining trials can be classified from the smallest to the highest cutting effect on fibre: $4 < 2 < 3 < 1 < 5 < 6$.

Hence, in a first approach, this range obtained can be compared with the different classifications already given by table *3*. The three last candidates for defining the refining intensity: the modified edge load *MEL*, the net tangential force per crossing point F_t^{net}/N_{CP}, the net normal force per crossing point F_n^{net}/N_{CP} succeed to evaluate the cutting effect on fibres.

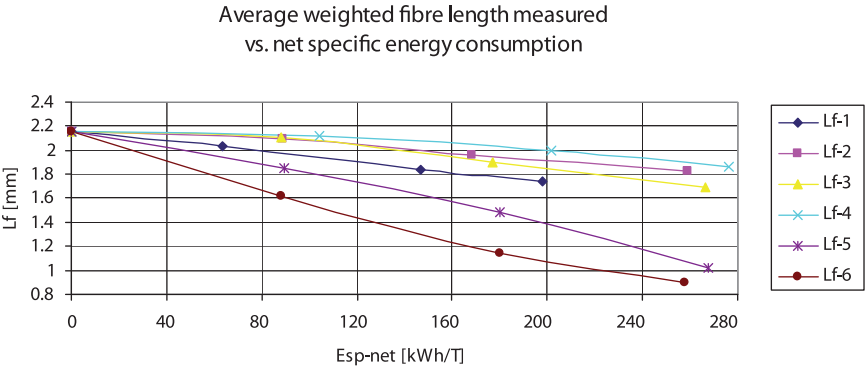

Figure 7. Experimental results for the six refining trials.

3.4 Benchmark of the different refining intensities

In order to determine the level of understanding which is obtained with one given refining intensity, we will compare the different average weighted fibre length (at *150 kWh/T*) for the six refining intensities.

A graphic interpretation will be privileged since it is the simplest one for performing the benchmark. In order to prepare the analysis, all the data are gathered in table 11.

We will show in the following developments the "clouds" of points between the different values of fibre length and that of refining intensity.

If we find a linear relationship between the fibre length and the corresponding refining intensity, it will mean that the refining intensity can be a good tool to quantifying the cutting effect on fibres.

Table 11. Data required for benchmarking the refining intensities

Trial n°	$L_{f-k}(150kWh/T)$ *[mm]*	B_s *[J/m]*	$B_{s\text{-}Tappi}$ *[J/m]*	*SSL* $[J/m^2]$	*MEL [J/m]*	F_t^{net}/N_{CP} *[N]*	F_n^{net}/N_{CP} *[N]*
1	1.841	0.656	0.672	202.7	3.299	1.737	11.58
2	2.001	0.380	0.388	117.2	1.908	1.005	5.58
3	1.978	1.067	1.167	205.1	2.426	1.466	7.33
4	2.073	0.623	0.681	119.7	1.415	0.855	3.42
5	1.610	1.103	1.129	227.1	5.545	2.919	22.45
6	1.290	2.135	2.185	439.6	10.73	5.651	35.32

Case of the specific edge load B_s

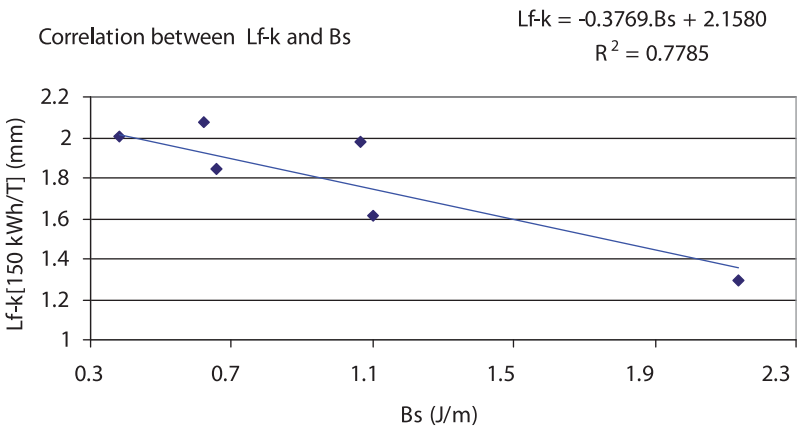

Figure 8. Correlation between the average weighted fibre length at $E_{sp}^{net} = 150\ kWh/T$ and the Specific Edge Load B_s.

Case of the specific edge load according to TAPPI engineering rules

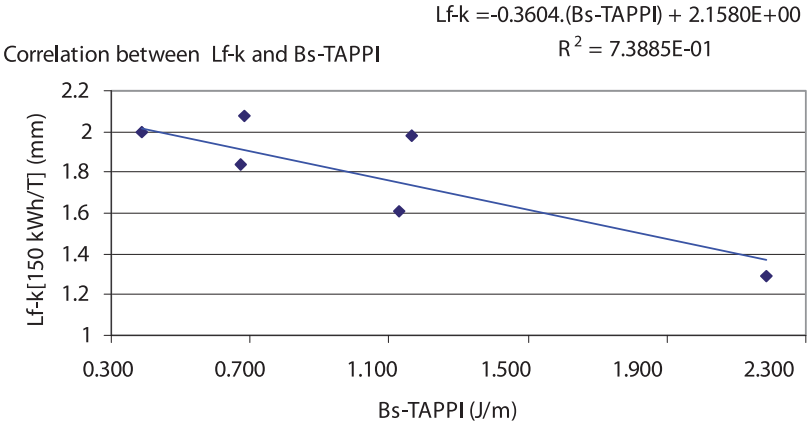

Figure 9. Correlation between the average weighted fibre length at $E_{sp}^{net} = 150\ kWh/T$ and the Specific Edge Load $B_{s\text{-}TAPPI}$.

At this point, neither the specific edge load nor its corrected value according to the TAPPI engineering rules is able to account for the understanding of the cutting kinetics on fibres. This result could have been observed in table 3 where the classification of the refining intensity was not in the same order as the cutting kinetics on fibres.

Hence, it could be adventurous to use in the paper industry these concepts alone to quantify the cutting effect on fibres.

Case of the specific surface load SSL

If the regression coefficient is better with the specific surface load than that with the two previous cases, it is also clear that the discriminating nature of this intensity is lost. At least, two pairs of fibre length cannot be discriminated with this tool as seen in figure 10.

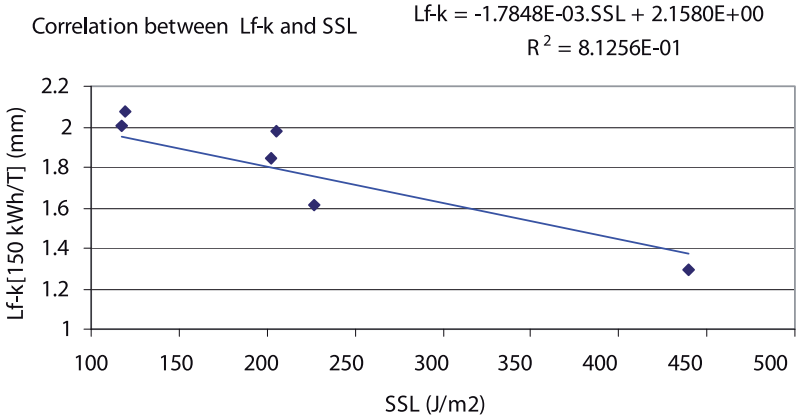

Figure 10. Correlation between the average weighted fibre length at $E_{sp}^{net} = 150\ kWh/T$ and the Specific Edge Load *SSL*.

Case of the modified edge load MEL

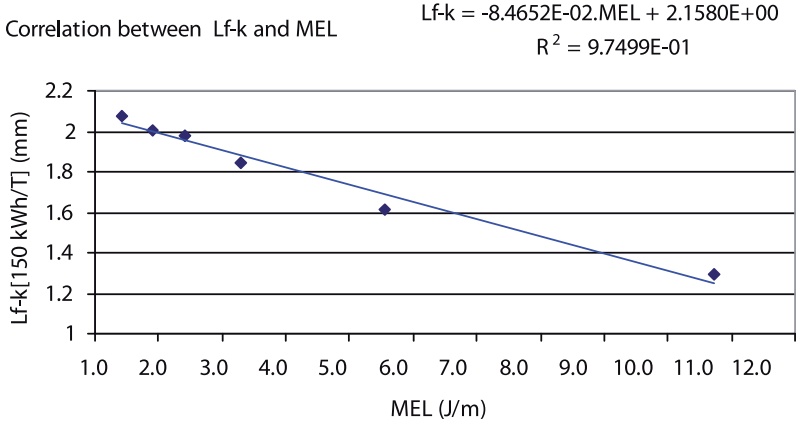

Figure 11. Correlation between the average weighted fibre length at $E_{sp}^{net} = 150\ kWh/T$ and the Modified Edge Load *MEL*.

Case of the net tangential force per crossing point F_t^{net}/N_{CP}

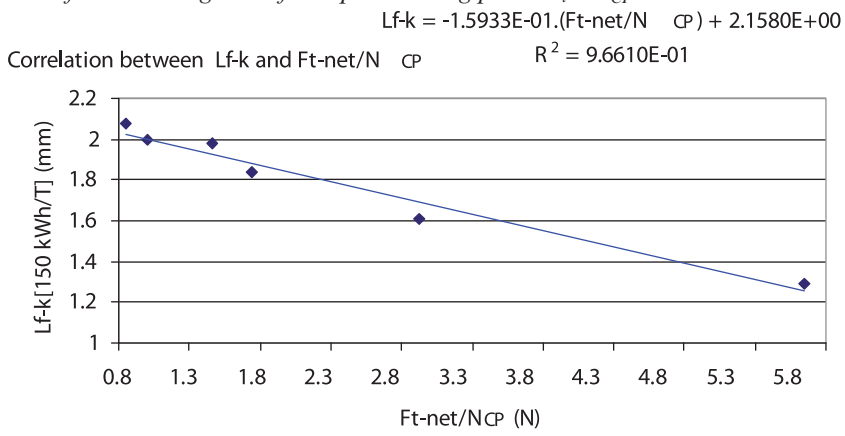

Figure 12. Correlation between the average weighted fibre length at E_{sp}^{net} = *150 kWh/T* and the net tangential force per crossing point F_t^{net}/N_{CP}.

Case of the net normal force per crossing point F_n^{net}/N_{CP}

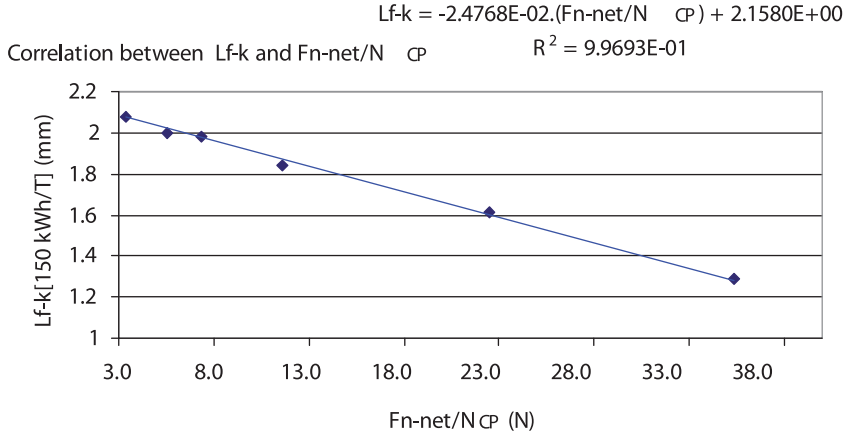

Figure 13. Correlation between the average weighted fibre length at E_{sp}^{net} = *150 kWh/T* and the net tangential force per crossing point F_n^{net}/N_{CP}.

As it was predicted from table 3 and from the experimental classification of the fibre length, the modified edge load, the net tangential force per crossing point and the net normal force per crossing point can be 3 success tools to quantify the cutting effect on fibres.

In this article, we have developed a unified physical refining theory which puts the emphasis on the net normal force per crossing point. Our reader is probably now convinced that this is the best refining intensity for the interpretation of the cutting kinetics on fibres. Even if the results with the net tangential force are acceptable, the introduction of the global friction coefficient is of primary importance in understanding the cutting effect on fibres.

We also have proved that the normal forces are responsible for the cutting on fibres and that the terminology often used in the industry of "cutting angle" should be eliminated definitely, we prefer to use crossing angle, which is exactly what it is, nothing more.

This classification of the cutting effect on fibres with these data is monotonous with the proposed refining intensity that is to say the net normal force per crossing point. The more the net normal force per crossing point, the more pronounced will be the cutting effect on fibres.

The average crossing angle is not the only influencing variable since the specific edge load on one hand and the global friction coefficient on the other hand counterbalance its effect, see equation (49) that is reminded in a simplified form:

$$\frac{F_n^{net}}{N_{CP}} \cong \frac{B_s}{f.sin(\bar{\gamma})} \tag{51}$$

When one wants to verify if a model takes correctly into account the experimental data, the parity diagram is an interesting tool for this purpose.

A parity diagram is given on figure 14 between the estimated fibre length

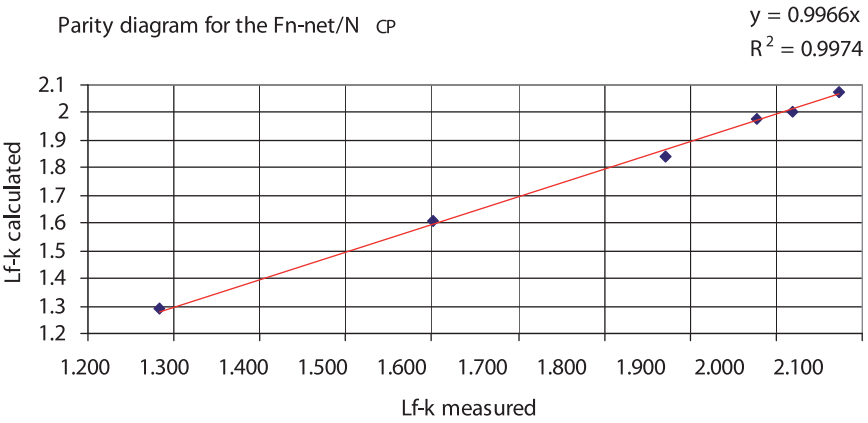

Figure 14. Parity diagram for the estimation of the average fibre length at *150 kWh/T* by using the net normal force per crossing point as refining intensity

and the measured fibre length (or the values interpolated when unknown directly). Hence, the knowledge of the refining intensity: the net normal force per crossing point is sufficient to quantify and predict the cutting effect on fibres.

CONCLUSIONS

In this article, we have proposed to revisit the earlier knowledge of the refining operation of pulp fibre suspension in low consistency range when it was operated on beater equipments.

By considering the relation between the cutting edge length and the bar contact area, two fundamental variables introduced previously by Jagenberg, it was possible to theoretically justify the extrapolations:

– in a first step, from a beater with parallel bars to a beater with inclined bars;
– in a second step, from a beater with inclined bars to a disc with inclined bars also.

This last extrapolation based initially on geometrical concepts was further justified by the physical analogy that exists between a slice of the beater and an elementary annulus of disc plates.

In the literature, it is possible to find different concepts for assessing the "refining intensity". A benchmark was undertaken considering the most famous practical refining intensities as the Specific Edge Load (B_s), its specific value according to the TAPPI engineering rules (B_s-*TAPPI*), the Specific Surface Load (*SSL*), the Modified Edge Load (*MEL*), the net tangential force per crossing point (F_t^{net}/N_{CP}) and the net normal force per crossing point (F_n^{net}/N_{CP}).

Six refining trials were carried out on our refining pilot under hydracycle conditions.

Two bar widths and two average bar crossing angles were investigated. These refining trials were compared considering the shortening effect on fibres at the same net specific energy consumption of *150 kWh/T*.

The results lead to the conclusion that three tools can be used as refining intensity to quantify the cutting effect on fibres: the modified edge load, the net tangential force per crossing point and the net normal force per crossing point. However, the net normal force per crossing point that results from our refining physical theory has the best monotonous variation with the shortening kinetics on fibres. It is graphically proved in this publication. All the other refining intensities were not sufficient in quantifying this shortening effect on fibres.

Another conclusion can be drawn from these results: the reference cumulative edge length and the cumulative edge length are definitely the same quantity. It is also the case for the reference specific edge load and the specific edge load which are identical. However, none of them include angular parameters

The specific edge load in fact is not sufficient to interpret the refining effects on fibres. Indeed, the global friction coefficient and at least the average crossing angle must be taken into account.

All these variables are considered in the net normal force per crossing point, a unified physical concept for correctly describing the intensity of the cutting on fibres, on equipments as different as beaters, disc or conical refiners.

BIBLIOGRAPHY

1. F. Jagenberg. **Das Höllandergeschirr in Briefen an einen Papiermacher**, 1887.
2. E. Kirchner. *Das Papier*. **4** Teil Ganzstoffe, 1906.
3. A. Pfarr. Holländer und deren Kraftverbrauch. *Wochenblatt für Papierfabrikation* **35**:3032–3039, 1907.
4. J.-C. Roux, J.-F. Bloch and P. Nortier. A kinetic model for pulp refining, including the angular parameters of the equipment. *Appita Journal* **60**(1):29–34, 2007.
5. C. Baker. **Refining Technology**, (ed. C. Baker), published by PIRA International Ltd, Leatherhead, 2000.
6. F. Meltzer. Key figures for the assessment of the refining process. Ch. 2 in **Refining Technology** (ed. C. Baker), PIRA International Ltd Publishing, Leatherhead, 2000.
7. F. Wultsch and W. Flucher. Der Escher-Wyss-Kleinrefiner als Standard-Prüfgerät für moderne Stoffaufbereitungsanlagen. *Das Papier* **13**(12):334–342, 1958.
8. W. Brecht and W.H. Siewert. Zür theorisch technischen Beurteilung des Mhlenprozesses moderner Mahlmaschinen. *Das Papier* **20**(1):4–14, 1966.
9. J.-C. Roux. Review Paper on pulp treatment processes. In **The Science of Papermaking,** *Trans. 12th Fund. Res. Symp.*, (ed. FRC), pp19–80, Oxford, 2001.
10. R. Bordin. Modélisation physique du fonctionnement d'un raffineur de pâte à papier: description hydrodynamique de l'action du raffineur sur les fibres, Ph-D thesis of Grenoble Institute of Technology, 2008.
11. R. Bordin, J.-C. Roux and J.-F. Bloch. Global description of refiner plate wear in low consistency beating. *Nordic Pulp and Paper Research Journal* **22**(4): 529–534, 2007.
12. R. Bordin, J.-C. Roux and J.-F. Bloch. New technique for measuring clearance in low-consistency refiners. *Appita Journal* **61**(1):71–77, 2008.
13. J. Lumiainen. New theory can improve practice. *Pulp and Paper International* **32**(8):46–54, 1990.

Transcription of Discussion

THE NET NORMAL FORCE PER CROSSING POINT: A UNIFIED CONCEPT FOR THE LOW CONSISTENCY REFINING OF PULP SUSPENSIONS

J.-C. Roux, J.-F. Bloch, R. Bordin and *P. Nortier*

Laboratoire de Génie des Procédés Papetiers, UMR CNRS 5518, Grenoble INP-Pagora, 461 rue de la Papeterie, 38402 Saint Martin d'Hères, France

Roger Gaudreault Cascades R&D

Why do you use the term "cutting kinetics" when you have not discussed the time effect? Surely, kinetics should involve time?

Jean-Claude Roux

We have presented a study at a net specific energy consumption of 150 kWh/tonne, but it is clear that the effect can be obtained also for any level of net specific energy. This means, on our installation, the time, because we are conducting constant net power trials. So we use the term "cutting kinetics".

Stefan Lindström Mid Sweden University

I was wondering what parameters do you need to keep constant in order to maintain this linear relation during refining? For example, moisture content and similar properties.

Jean-Claude Roux

If I correctly understand your question, we have a line where all the points are aligned only due to the fact that the refining intensity reveals the physical

phenomena in the cutting kinetics of fibres. In statistics when you have an uncertainty on a typical phenomenon, you have clouds of points which are spread out. If you manage to properly understand the system, you will restrict the clouds to a line. It is the purpose of my graphical comparison. If our tool is a correct tool for understanding the kinetic phenomena, then all points should be aligned. We will have obtained a relationship between output and input.

Stefan Lindström

Yes, I understand but what if you changed something else like the contents of moisture in the system, or the geometry: would the linear relation still hold?

Jean-Claude Roux

If you change, for example, the bar crossing angle, this will have an effect on the formula because it will change the net normal force per crossing point. Suppose you change the metal of the bars by changing plates, this will produce a change of the global friction coefficient. Suppose, you used wounded bars or sharp bars, this will produce a change of the global friction coefficient. So we believe that actually we have the knowledge of the phenomena with this formula. If you change, for example, the consistency, you will get also a change in the global friction coefficient. This global friction coefficient is a concept which seems very powerful for describing refining effects on fibres. I have presented to you only the results on cutting effects, but we could also use the concept to explain hydration, with the WRV, or the Schopper-Riegler level of the pulp.

Warren Batchelor Monash University (from the chair)

It was not quite clear to me how you are measuring the global friction coefficient?

Jean-Claude Roux

That is a very difficult question. The global friction coefficient in fact can be determined from the net power, but also, in the calculation we presented, from the normal force. So, our refining installation is equipped with a specific sensor for the normal force. At the beginning, I studied refining phenomena as hydrodynamical and I was very interested by the load, which is exactly the same as the load with the plane. It is a bearing load which is in fact very close

to phenomena that we find in hydrodynamics, making it very important. Another important quantity of course is the gap clearance. We have presented a lot of publications on this subject, it is very difficult to measure.

Juha Salmela VTT

You are using net power. You have friction and other losses. Have you thought about measuring directly the forces on the gap or on the bar itself?

Jean-Claude Roux

Good question. In fact, we have measured both. We measured on the axis, on the shaft, but we also have seen the distribution of the normal force in the corona, in the annulus. It is a very important point because from the input to the output of the disk element annulus, you have different forces which are exerted on fibres, and different refining intensity. So, we have proposed only one refining intensity but in fact the raw material receives a distribution of refining intensity inside the disc annulus. So, as you can see, the area is open for future work, many years of research, and many publications.

Wolfgang Bauer Graz University of Technology

Could we just go back to the parity diagram again, because I did not fully understand how you calculated the average fibre length shown in the diagram?

Jean-Claude Roux

The parity diagram (figure 14 in the paper in the proceedings, ed.) compares the calculated fibre length (with net normal force per crossing point as an estimate of refining intensity) and measured length. You will recall that, for each refining intensity, the model which seems to be a good candidate for our data is a parabolic curve for the variation of fibre length with net specific energy consumption. So, for trial number k (at one refining intensity), we have two coefficients a_k and b_k which can be determined, allowing us to interpolate a fibre length at 150 kWh/tonne. This calculated fibre length allows us to see directly the refining intensity. We know the refining intensity for each trial using several different measures, and we can plot these against the calculated fibre lengths. That is why we produce the parity diagram, to compare this straight-line model of fibre length with the measured values. We can produce it with the other measures of refining intensity, but it does not work so well.